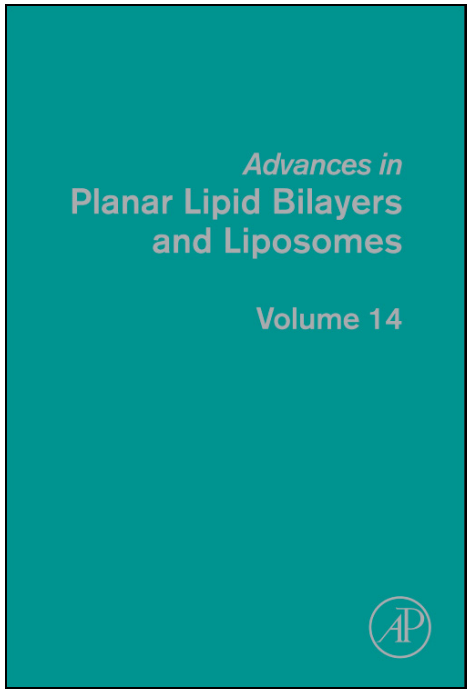

From: F. Ziebert and D. Lacoste, A Planar Lipid Bilayer in an Electric Field: Membrane Instability, Flow Field, and Electrical Impedance. In Aleš Iglič, editor: Advances in Planar Lipid Bilayers and Liposomes, Vol. 14,
Burlington: Academic Press, 2011, pp. 63-95.
ISBN: 978-0-12-387720-8

CHAPTER THREE

A Planar Lipid Bilayer in an Electric Field: Membrane Instability, Flow Field, and Electrical Impedance

F. Ziebert[1,2,3] *and* D. Lacoste[1,*]

Contents

* Corresponding author. Tel.: +33-140-795140; Fax: +33-140-794731.
E-mail address: david.lacoste@gmail.com

[1] Laboratoire de Physico-Chimie Théorique - UMR CNRS Gulliver 7083, ESPCI, 10 rue Vauquelin, Paris, France
[2] Physikalisches Institut, Albert-Ludwigs-Universität, Freiburg, Germany
[3] Institut Charles Sadron, 23 rue du Loess, Strasbourg, France

Advances in Planar Lipid Bilayers and Liposomes, Volume 14
ISSN 1554-4516, DOI: 10.1016/B978-0-12-387720-8.00003-0

Abstract

For many biotechnological applications it would be useful to better understand the effects produced by electric fields on lipid membranes. This review discusses several aspects of the electrostatic properties of a planar lipid membrane with its surrounding electrolyte in a normal DC or AC electric field.

In the planar geometry, the analysis of electrokinetic equations can be carried out quite far, allowing to characterize analytically the steady state and the dynamics of the charge accumulation in the Debye layers, which results from the application of the electric field. For a conductive membrane in an applied DC electric field, we characterize the corrections to the elastic moduli, the appearance of a membrane undulation instability and the associated flows which are built up near the membrane. For a membrane in an applied AC electric field, we analytically derive the impedance from the underlying electrokinetic equations. We discuss different relevant effects due to the membrane conductivity or due to the bulk diffusion coefficients of the ions. Of particular interest is the case where the membrane has selective conductivity for only one type of ion. These results, and future extensions thereof, should be useful for the interpretation of impedance spectroscopy data used to characterize, for example, ion channels embedded in planar bilayers.

1. Introduction

Bilayer membranes formed from phospholipid molecules are an essential component of the membranes of cells. The mechanical properties of equilibrium membranes are characterized by two elastic moduli, the surface tension and the curvature modulus [1], which typically depend on the electrostatic properties of the membranes and its surroundings [2]. Understanding how these properties are modified when the membrane is driven out of equilibrium is a problem of considerable importance to the physics of living cells. A membrane can be driven out of equilibrium in many ways, for instance by ion concentration gradients or by electric fields.

Quite generally one can distinguish between systems in which the electric field is applied externally and systems which are able to self-generate electric fields.

1.1. Membranes in Externally Applied Electric Fields

The external application of electric fields on lipid films is used to produce artificial vesicles (electroformation), as well as to create holes in the membrane (electroporation) [3]. Both processes are important for biotechnological applications and they are widely used experimentally. However, they are still not well understood theoretically. The research on electroformation is motivated by the hope to produce artificial lipid vesicles in a controlled

and simple way, which will be key to many biotechnological applications. Cell electroporation is a popular technology and biomedical applications of *in vivo* cell electropermeabilization [4] are gaining momentum for drug and nucleic acids electrotransfer and for the destruction of tumor cells for cancer treatment [5].

In view of the importance of these applications, many research efforts have been devoted to study and understand deformations of giant unilamellar vesicles (GUVs) due to the application of electric fields. In the presence of an AC electric field, GUVs show a rich panel of possible behaviors and morphological transitions depending on experimental conditions—electric field frequency, conductivities of the medium and of the membrane, salt concentration, etc., [6,7]. A theoretical framework involving hydrodynamics and a continuum mechanics description of the membrane has been developed, which accounts quantitatively for the observed equilibrium and nonequilibrium shapes taken by the vesicles in the presence of an AC electric field [8,9]. For a clear and self-contained presentation of this theoretical framework, we recommend the chapter "Non-equilibrium dynamics of lipid membranes: deformation and stability in electric fields" by P. Vlahovska [53].

The application of external fields is also interesting as a means to move fluids via electro-osmosis [10,11] and to self-assemble colloidal particles, for various technological applications. Moreover, the ability to move fluids and nanoparticles at small scales is used in many biological systems. For instance, membrane-bound ion pumps and channels are able to transport water (for instance in aquaporin channels) and ions (in ionic pumps and channels) in a particularly selective and efficient way, which one would like to reproduce in artificial or biomimetic microfluidic devices.

1.2. Membranes in Self-generated Electric Fields

In some cases of biological relevance, membranes are able to self-generate an electric field, due to embedded ion channels or pumps. This can be achieved because the channels are able to transport ions from one side of the membrane to the other in a selective way, either down their concentration gradient in passive transport or against it in active transport, for example, coupled to the hydrolysis of Adenosine triphosphate or activated by light. Probably the best known example is the opening and closing of ion channels in nerve cells allowing the transmission of an electric signal via action potentials [12]. For all these reasons, ion channels and pumps play an essential role in many biological functions of a cell [13].

In order to better understand how nerve cells operate *in vivo*, it would be helpful to construct an in vitro biomimetic equivalent which would have some key features of the *in vivo* system, such as the ability to generate an action potential, but without the complexity of a real nerve cell. Active

membranes, which are GUVs containing ion pumps such as bacteriorhodopsin [14–16] are a promising system to achieve this goal.

The main purpose of this review is to propose and analyze a simple model to foster the understanding of various effects resulting from electric fields acting on a planar lipid membrane. Although we are mostly interested in applications to biological or biomimetic systems composed of lipid membranes, we would like to point out that the theoretical framework presented here is very general. It can be easily adapted to analyze the electrical properties of artificial membranes which can have very different properties from biological membranes (as far as, e.g., ionic conductivities or the bending stiffness are concerned).

This review is organized as follows: in Section 2 we present the model for a planar lipid membrane and its surrounding fluid in an applied electric field. In this section, we will restrict ourselves to the case of a DC field. In particular we will focus on (i) the electrostatic and electrokinetic steady-state corrections to the elastic moduli of the membrane due to the application of the electric field, see Section 2.3; (ii) the flow fields which can be predicted from such an approach, at steady state and in the case that the membrane is ion-conductive, see Section 2.4. In Section 2.5 we will compare the model predictions to two relevant experiments. More details on this theoretical framework, as well as an extension to the nonlinear electrostatic regime using the Poisson–Boltzmann (PB) equation, can be found in Refs. [17–20]. Finally, in Section 3 we present an analysis of the model in the presence of time-dependent AC electric fields. We provide derivations for the impedance of the system from the underlying electrokinetic equations, for situations where the membrane is either blocking or selectively conductive for ions.

2. A Quasi-Planar Membrane in a DC Electric Field

The mechanical properties of membranes at equilibrium are characterized by two elastic moduli, the surface tension and the bending modulus. These moduli typically depend on electrostatic properties, and their modifications in the case of charged membranes or surfaces in an electrolyte have been examined theoretically in various situations: in the linearized Debye–Hückel approximation as well as in the nonlinear PB regime, for lipid monolayers and symmetric bilayers [2,21–23]. More recently, charged asymmetric bilayers with unequal Debye lengths on both sides of the membrane [24] and an uncharged membrane in a DC field [25] have been investigated.

In all the works mentioned above, a free energy approach has been used. Note that while this method works well for equilibrium membranes, it is not applicable to situations in which the membrane fluctuations have a nonequilibrium origin, as in the case of active membranes containing ion channels [14,15,26,27] or in the case of a membrane in a time-dependent electric field. In our recent work [17–20], we thus have studied this problem using an electrokinetic approach, which does not have the limitations of a free energy formulation. In this framework we allow for a finite conductivity of the membrane due to, for example, ion channels or pumps, and the ion transport is described using a Poisson–Nernst-Planck (PNP) approach [28–30]. The electrostatic corrections to the elastic moduli and the fluid flows in the electrolyte are then obtained by imposing the overall force balance at the membrane.

Two additional points are worth emphasizing: first, our approach is able to correctly describe the capacitive effects of the membrane and of the Debye layers while keeping the simplicity of the "zero-thickness approximation" on which most of the literature on lipid membranes is based. This is accomplished by the use of an effective Robin-type boundary condition (BC) at the membrane. Second, as the method is based on a calculation of the general force balance at the membrane, additional nonequilibrium processes could be included into the model rather easily. For simplicity we investigate here only the effects of ionic currents flowing through the membrane, which in turn affect the fluid flow near the membrane. Other nonequilibrium effects that could be included as well are for instance ion channel stochasticity or active pumping.

2.1. Model Equations: Electrostatics

Figure 1 shows a sketch of the planar geometry that is studied: we consider a steady current driven by a DC voltage drop V across two electrodes separated by a fixed distance L. The membrane is quasi-planar and located at $z = 0$. It is embedded in an electrolyte of monovalent ions with number densities n^+ and n^-. It contains channels for both ion species but is itself neutral, that is, does not carry fixed charges. The channels or pumps are assumed to be homogeneously distributed in the membrane and enter only in the effective conductance G, as introduced below. A point in the membrane is characterized in the Monge representation by the height function $h(\mathbf{r}_\perp)$, where $\mathbf{r}_\perp$ is a two-dimensional in-plane vector. The base state of this problem is a flat membrane. Hence the electric field, assumed to be perfectly aligned in z-direction, is perpendicular to it. We assume a quasi-static approach [18,25] in which membrane fluctuations are much slower than the characteristic diffusion time $\tau = 1/D\kappa^2$ for the ions to diffuse a Debye length.

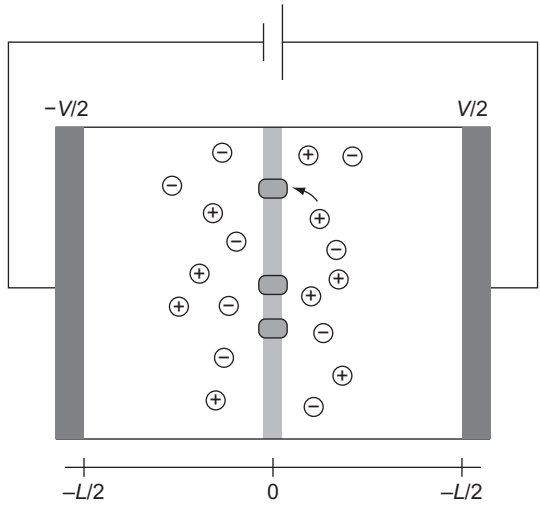

Figure 1 Sketch of a quasi-planar membrane embedded in a symmetric electrolyte. The initially flat bilayer membrane is represented by the plane $z = 0$. The membrane fluctuations around this base state have not been represented. A voltage $\pm V/2$ is applied on each electrode, which are separated by a distance L. The membrane carries ion channels which give rise to a conductance G.

In the electrolyte, the electric potential ϕ obeys Poisson's equation

$$\nabla^2\phi = -\frac{1}{\varepsilon}(en^+ - en^-) = -\frac{2}{\varepsilon}\rho. \tag{1}$$

Here e is the elementary charge, ε is the dielectric constant of the electrolyte and we have introduced *half* of the charge density,

$$\rho = e\frac{n^+ - n^-}{2}. \tag{2}$$

For the sake of simplicity, we assumed a symmetric 1:1 electrolyte, thus far away from the membrane $n^+ = n^- = n^\star$, and the total system is electrically neutral. The densities of the ion species obey the PNP equations

$$\partial_t n^\pm + \nabla\cdot\mathbf{j}^\pm = 0, \quad \mathbf{j}^\pm = D\left(-\nabla n^\pm \mp n^\pm \frac{e}{k_\mathrm{B}\mathrm{T}}\nabla\phi\right), \tag{3}$$

where $\mathbf{j}^\pm$ are the particle current densities of the ions and $k_\mathrm{B}T$ is the thermal energy. We will assume here that both ion types have the same diffusion coefficient D. Note that we will discuss the effects of differing diffusion coefficients for an applied AC voltage in Section 3.4.

Since we are primarily interested in the behavior close to the membrane, for the BCs far away from the membrane we assume

$$\phi(z = \pm L/2) = \pm V/2, \tag{4}$$

$$\rho(z = \pm L/2) = 0. \tag{5}$$

Equation (4) states that the potential at the electrodes is held fixed externally. This BC is quite oversimplified for real electrodes, but captures the main effects of the electric field, see the discussion in Ref. [19]. We have also assumed that the distance between the electrodes is much larger than the Debye length, $L \gg \lambda_D = \kappa^{-1}$, where

$$\kappa = \sqrt{\frac{2e^2 n^*}{\varepsilon k_B T}} = \lambda_D^{-1}. \tag{6}$$

Hence, as already mentioned above, the bulk electrolyte is quasi-neutral with negligible charge density (compared to the total salt concentration) and far from the membrane Eq. (5) holds.

The BC at the membrane is crucial to correctly account for capacitive effects. We use the Robin-type BC (see Appendix for a derivation)

$$\lambda_m(\mathbf{n}\cdot\nabla)\phi_{|z=h^+} = \lambda_m(\mathbf{n}\cdot\nabla)\phi_{|z=h^-} = \phi(h^+) - \phi(h^-), \tag{7}$$

where $\mathbf{n}$ is the unit vector normal to the membrane and

$$\lambda_m = \frac{\varepsilon}{\varepsilon_m} d. \tag{8}$$

λ_m is a length scale containing the membrane thickness d and the ratio of the dielectric constants $\varepsilon/\varepsilon_m$ of the electrolyte and the membrane. Note that in Eq. (7), the membrane plays a similar role as the Stern layer in the description of Debye layers near a charged interface. This BC was rederived for electrodes sustaining Faradaic current [31,32] or charging capacitively [33], and was applied for membranes in Refs. [18,19,30]. There it was shown to properly account for the jump in the charge distribution which occurs near the membrane as a result of the dielectric mismatch between the membrane and the surrounding electrolyte.

In addition to Eq. (7), we impose the continuity of the bulk current $j^\rho_{|z=0}$ at the membrane. This BC involves the ohmic law

$$j^\rho_{|z=0} = -\frac{G}{e}[\mu^\rho]_{z=0}, \tag{9}$$

where G denotes the membrane conductance per area and μ^{ρ} the electrochemical potential. The electrostatic potential and the ion densities can now be obtained by solving Eqs. (1, 2) in the linear Debye–Hückel approximation and one obtains [19]:

(i) the jump of the charge density at the membrane, ρ_m,
(ii) the current through the membrane, j_m, and
(iii) the electric field inside the membrane, E_0^m:

$$\rho_m = \frac{(\varepsilon\kappa^2/2)V - (j_m/D)(L+\lambda_m)}{2+\kappa\lambda_m}, \tag{10}$$

$$j_m = -j^{\rho} = \frac{GV}{1+(2/\varepsilon\kappa^2 D)GL}, \tag{11}$$

$$E_0^m = -\frac{1}{d}\left[\frac{2}{\varepsilon\kappa^2}\left(-\frac{j_m L}{D} - 2\rho_m\right) + V\right]. \tag{12}$$

For simplicity, in the derivation of Eqs. (10)–(12) we assumed equal ion conductivities ($G^+ = G^- = G$) and a symmetric electrolyte on both sides of the membrane ($\kappa^{>0} = \kappa^{<0} = \kappa$). Note that the method presented in this section can be easily extended to cover more general cases. In addition, the nonlinear electrostatic problem (keeping the PB equation) can be still solved analytically in the non-conductive case. The nonlinear generalizations of Eqs. (10)–(12) can be found in Ref. [20].

2.2. Model Equations: Hydrodynamics and Force Balance at the Membrane

The hydrodynamics of the electrolyte is described by the incompressible Stokes equation, $-\nabla p + \eta\nabla^2 \mathrm{v} + \mathbf{f} = 0$ with $\nabla \cdot \mathbf{v} = 0$, where $\mathbf{v}$ is the velocity field of the electrolyte, η its viscosity, p the hydrostatic pressure and $\mathbf{f} = -2\rho\nabla\phi$ the electric driving force. From the solution of the electrostatic and the hydrodynamic problem, one obtains the total stress tensor

$$\tau_{ij} = -p\delta_{ij} + \eta\left(\partial_i v_j + \partial_j v_j\right) + \varepsilon\left(E_i E_j - \frac{1}{2}\delta_{ij}E^2\right), \tag{13}$$

which contains the pressure, the viscous stresses in the fluid and the Maxwell stresses.

The lipid bilayer membrane, on the other hand, behaves as a two-dimensional fluid which can store elastic energy in bending deformations.

More precisely, its elastic properties can be described by the standard Helfrich free energy

$$F_{\mathrm{H}} = \frac{1}{2}\int d^2\mathbf{r}_\perp \left[\Sigma_0(\nabla h)^2 + K_0\left(\nabla^2 h\right)^2\right], \tag{14}$$

where Σ_0 is the bare surface tension and K_0 the bare bending modulus of the membrane.

All forces present in the system, the electrostatic, viscous, and elastic ones, have to fulfill the force balance equation. The latter states that the discontinuity of the normal–normal component of the stress tensor, as defined in Eq. (13) and evaluated at the membrane position, must equal the restoring force due to membrane elasticity, hence

$$-\left(\tau_{z\,z,1|z=h^+} - \tau_{zz,1|z=h^-}\right) = -\frac{\partial F_{\mathrm{H}}}{\partial h(\mathbf{r}_\perp)} = \left(-\Sigma_0 k_\perp^2 - K_0 k_\perp^4\right) h(\mathbf{k}_\perp)\cdot \tag{15}$$

Here the index 1 in the stress tensor refers to the order of an expansion with respect to the membrane height field $h(\mathbf{r}_\perp)$. Note that at zeroth order, the membrane is flat and thus only electric forces and osmotic pressure balance. By expanding to linear order in the height field $h(\mathbf{r}_\perp)$, and using

$$h \propto h_0 \mathrm{e}^{i\mathbf{k}_\perp\cdot\mathbf{r}_\perp + s(\mathbf{k}_\perp)t}, \tag{16}$$

Equation (15) yields the growth rate $s(\mathbf{k}_\perp)$ of membrane fluctuations. Details of the derivation of $s(\mathbf{k}_\perp)$ can be found in Refs. [17–19]. We would like to emphasize that the force localized at the membrane surface is a priori unknown in this problem. Thus it must be determined self-consistently from the BCs for the velocity and the stress.

2.3. Growth Rate and Renormalized Elastic Moduli

The force balance Eq. (15) determines the growth rate $s(\mathbf{k}_\perp)$ entering the normal stress difference,

$$\eta k_\perp s(\mathbf{k}_\perp) = -\frac{1}{4}(\Sigma_0 + \Delta\Sigma)k_\perp^2 - \Gamma_\kappa k_\perp^3 - \frac{1}{4}(K_0 + \Delta K)k_\perp^4\cdot \tag{17}$$

The electrostatic corrections to the surface tension, $\Delta\Sigma = \Delta\Sigma_\kappa + \Delta\Sigma_m$, and to the bending modulus, $\Delta K = \Delta K_\kappa + \Delta K_m$ can be decomposed into:

(i) an outside contribution due to the charges accumulated in the Debye layers and denoted with the index κ;

(ii) an inside contribution due to the voltage drop at the membrane and denoted with an index m. They are given by

$$\Delta\Sigma_\kappa = -4\frac{\rho_m^2}{\varepsilon\kappa^3} - 16\frac{\rho_m j_m}{\varepsilon\kappa^4 D}, \quad \Delta K_\kappa = \frac{3\rho_m^2}{\varepsilon\kappa^5} \tag{18}$$

for the contribution due to the Debye layers and by

$$\Delta\Sigma_m = -\varepsilon_m\left(E_0^m\right)^2 d, \quad \Delta K_m = \varepsilon_m\left(E_0^m\right)^2\left(\frac{d^3}{12} - \frac{\rho_m}{E_0^m}\frac{d}{\varepsilon\kappa^3}\right) \tag{19}$$

for the contribution due to the field inside the membrane.

Note that in Eq. (17), one also obtains a purely nonequilibrium correction $\Gamma_\kappa = (4\rho_m j_m)/(\varepsilon\kappa^5 D)$. It would correspond to a term proportional to $k_\perp^3$ in an "effective membrane free energy" incorporating the Maxwell stresses. At equilibrium such a term is forbidden by symmetry, but in a nonequilibrium situation, where the membrane sustains a current $j_m \neq 0$, it is allowed. For realistic parameters, however, this term is very small, see Ref. [18] for a detailed discussion.

The inside contribution to the membrane surface tension is always negative, see Eq. (19). The same is typically true for the outside contribution, see Eq. (18) and note that $\rho_m, j_m > 0$. Hence these contributions can overcome the bare surface tension Σ_0. If this is the case, an instability towards membrane undulations sets in. Such an instability had already been described for the high salt limit in Ref. [34]. Note that the linearized theory developed here describes only the early stages of the instability, but it is more general than previous works since it is not limited to the high salt limit and in addition accounts for hydrodynamic effects. The linear growth rate of the membrane fluctuations given by Eq. (17) is shown in Fig. 2 in rescaled units. We scaled the wave vector by κ, hence $k' = k_\perp/\kappa$ and the time by the typical time for ions to diffuse a Debye length, $\tau = 1/D\kappa^2$. The control parameter of the instability is the external voltage V. Figure 2 shows the growth rate for three different levels of the voltage: the dashed line is for $V = 0.7$ V, which lies below the threshold of the instability, all wave numbers are damped and the membrane is stable. The solid and the dash-dotted line correspond to $V = 0.75$ and 0.8 V. These values are above threshold and the growth rate is positive for a finite wave number window.

For a more detailed discussion of the dependence of the corrections to the elastic moduli, the instability threshold and the characteristic wave number as a function of salt concentration and membrane conductivity, we refer the reader to Refs. [18,19].

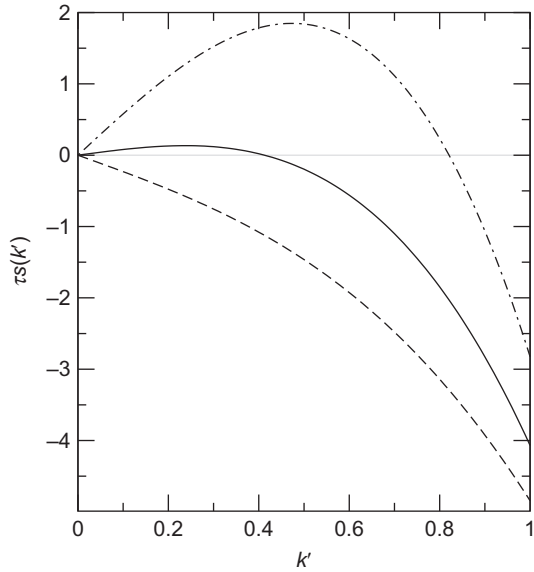

Figure 2 The renormalized growth rate or dispersion relation, τs, as a function of the rescaled wave number $k' = k_\perp/\kappa$ for three voltages: $V = 0.7$ V (dashed line), $V = 0.75$ V (solid line), and $V = 0.8$ V (dash-dotted line). We have used the following parameters: dielectric constants $\varepsilon = 80\varepsilon_0$ and $\varepsilon_m = 2\varepsilon_0$; membrane thickness $d = 5$ nm leading to $\lambda_m = (\varepsilon/\varepsilon_m)d = 200$ nm; diffusion coefficient of ions $D = 10^{-9}\text{m}^2\text{s}^{-1}$; viscosity $\eta = 10^{-3}$ Pas; inverse Debye length $\kappa = 2 \times 10^7$ m^{-1}; bare surface tension $\Sigma_0 = 1$ mN m^{-1}; bare bending modulus $K_0 = 10\ k_\text{B}T$. Here we assumed a non-conductive membrane, $G = 0$.

2.4. Flow Fields Near a Driven Membrane

We now summarize the main features of the fluid flows which arise near the membrane when it is driven by ionic currents [18]. Figure 3 was generated by selecting the fastest growing wave number and using the corresponding maximum growth rate. The shape of the membrane undulation is represented with the black solid curves. Figure 3C shows the flow field for a high membrane conductance and low salt, in the regime where the membrane is unstable due to the electrostatic correction to the surface tension and thus starts to undulate. The resulting flow is a superposition of two distinct flows: first, the typical flow associated to a membrane bending mode [35] as shown in Fig. 3A. Second, the flow which results from the ion transport across the membrane. The latter flow has the typical counter-rotating vortices of an ICEO flow [36], as shown in Fig. 3B. Clearly, the superposition of these two flow contributions, Fig. 3C, results in a parallel flow close to the membrane, in contrast to the usual bending mode flow given by Fig. 3A.

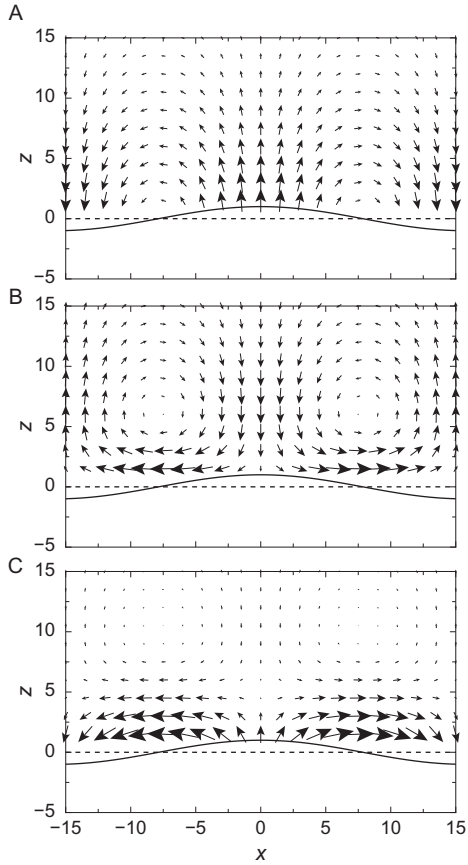

Figure 3 Representation of the flows around the membrane beyond the instability threshold. The orientation of the electric field is toward negative values of z. (A) shows the flow generated by the membrane bending mode. (B) shows the ICEO flow. Finally, (C) shows the actual flow, which is the superposition of the former two and results in a strong flow near the membrane, oriented parallel to the surface. Both axes are scaled by the Debye length κ^{-1}. Parameters are as in Fig. 2 except $V = 3.165$ V, $\kappa = 10^7$ m^{-1}, $G = 10$ Sm^{-2} and $L = 10$ μm.

For most realistic parameters—modest conductivities, not too low salt—the flow generated by membrane bending is usually dominating and hides the small ICEO contribution. To be able to observe the flows of Fig. 3, a high membrane conductance G and low salt are needed. Also, since for macroscopic electrode distances L (e.g., of the order of millimeters), the voltage needed to induce the instability is very high, we have assumed a microscopic electrode distance of $L = 10$ μm. While it might still be possible to observe flows for higher salt and macroscopic electrode

separations, such situations cannot be analyzed within the Debye–Hückel approximation used here.

Note that somewhat similar looking flow patterns have been recently observed experimentally in vesicles subject to AC electric fields in Ref. [6]. On closer inspection, however, it appears that these flows most probably have a different origin from the ICEO flows, since they are more likely to result from electrophoresis of charged lipids within the membrane.

2.5. Applications to Specific Experiments

Here we will briefly discuss how the framework presented above can be applied to recent experiments: the first experiment studied supported membranes subject to an electric field [37], while the second one investigated active membranes [14–16].

Lecuyer *et al.* [37] recently performed neutron reflectivity measurements on a system consisting of two nearby membrane bilayers in an external AC electric field. One of the bilayers was close to the bottom electrode and used to protect the second one from interacting with the wall. The bare values of the elastic moduli were known from X-ray off-specular experiments for a similar system [38], yielding $\Sigma_0 \simeq 0.5$ mN m^{-1} and $K_0 \simeq 15\ k_B T$. The experiments were performed in an AC electric field at several frequencies. For the lowest frequency (10 Hz) and for a voltage of $V = 5$ V, the electrostatic corrections to the surface tension and bending modulus were found to be $\Delta\Sigma \simeq -1 \pm 0.15$ mN m^{-1} and $\Delta K \simeq 185 \pm 15\ k_B T$.

Assuming that the membrane is non-conductive, $G = 0$, and using an inverse Debye length of $\kappa = 2 \times 10^7$ m^{-1} (milli-Q water) and the experimental electrode distance of $L = 1$ mm, our model yields $\Delta\Sigma \simeq -2$ mN m^{-1} and $\Delta K \simeq 190\ k_B T$. Thus the model successfully accounts for the order of magnitude of the electrostatic corrections observed in this experiment. Note, however, that the linearized Debye–Hückel approach is not a good approximation in this case, as applied voltages are rather high. For this reason, we recently extended our work to the PB regime [20].

The second experiments we would like to discuss concerns active membranes, which are artificial lipid vesicles containing bacteriorhodopsin ionic pumps [14–16]. These pumps are able to transfer protons unidirectionally across the membrane by undergoing light-activated conformational changes. The transport of protons across the membrane eventually builds up a transmembrane potential. In Refs. [15,26,27], a hydrodynamic theory has been developed to describe the nonequilibrium fluctuations of the membrane induced by the activity of the pumps. This work triggered substantial theoretical interest in the problem, mainly focusing on the proper description for these nonequilibrium effects associated with protein conformational changes [39–43].

In these models for active membranes, the electrostatic effects associated with the ion transport were not explicitly described. The framework presented in this review provides a more detailed description of the ion transport, which could be useful to understand some aspects of active membrane experiments. From a contour analysis of giant active vesicles, the fluctuation spectrum of the membrane was measured in Ref. [16], and a lowering of the membrane tension produced by the activity of the pumps was reported. Only the correction to the surface tension has been accurately measured in this experiment and many aspects of the transport of ions are still unknown. However, for simplicity we can assume that the passive state corresponds to a non-conductive membrane, $G = 0$, and the active state to a membrane with conductance $G = 10\ Sm^{-2}$. If we also assume a typical transmembrane potential of the order of 50 mV, we can use the results for the corrections to the surface tension obtained above. Accounting for the rather high amount of salt using $\kappa \simeq 5 \times 10^8\ m^{-1}$, we find a reasonable estimate for the observed tension lowering, $\Delta\Sigma \simeq 3 \times 10^{-7}\ Nm^{-1}$. We also find that there is no measurable difference for the bending modulus between the active and passive state, in agreement with the experiments. The model further predicts a current density of $j_m \simeq 1\ Am^{-2}$ when the pumps are active, which corresponds to an overall current of 1 pA on a vesicle of size 1 μm.

This accord in orders of magnitude for the electrostatic corrections is quite promising. For a more detailed comparison between experiments and the presented model, it would be necessary to do experiments in varying conditions (ionic strength, conductance of the membrane, or orientation of the pumps in the membrane for instance). Combined measurements of the membrane current and the transmembrane potential in the same experiment, using, for example, patch-clamp techniques, would also be desirable.

3. Impedance of a Planar Membrane in an AC Electric Field

Impedance spectroscopy [44] is an effective tool to obtain a characterization of the electric properties of lipid bilayer membranes. The method has been used in particular for supported lipid bilayers, which are a promising experimental system to characterize membrane proteins, channels or inclusions and more generally constitute the basis of highly sensitive detection technologies, that is, biosensors [45]. In the recent work [46], for instance, impedance spectroscopy has been used to characterize gramicidin D channels in pore suspending membranes. Nowadays, many biotechnology companies develop systems to measure the impedance of whole cells for screening or drug delivery.

In many cases, the interpretation of the data obtained by impedance spectroscopy is not that straightforward. Typically one uses equivalent circuits, which are sometimes controversial, since different models can be used for fitting the data. Moreover, there is often a lack of knowledge concerning the conditions of validity of these equivalent circuits to describe the diffuse charging in electric Debye layers. To answer these questions, one possibility is to start with an electrokinetic description based on the PNP equations. With such an approach, the dynamics of diffuse charging [33] and the current–voltage relation in electrochemical thin films have been successfully analyzed [32]. This approach is also useful for relating impedance measurements to the properties of the diffuse layers near charge selective interfaces such as electrodes or ion-exchange membranes [47].

In the following, we extend the model studied in the previous sections to the case of an applied AC electric field. For simplicity the membrane will be assumed to be *strictly planar and non-fluctuating*. We use the PNP equations to evaluate the impedance of this system, which can be then compared to simple equivalent circuits. We will first present the generic time-dependent equations for the perturbation induced by the applied AC field. Then we proceed to calculate the impedance for the following cases: (i) an ideally blocking membrane with equal diffusion coefficients for the two ion species, (ii) the same system but with unequal ion diffusion coefficients and finally (iii) an ideally non-blocking membrane which conducts selectively only one type of ion.

3.1. Time-dependent Electric Fields

The PNP equations for an electrolyte have already been given in Section 2.1. Taking the time derivative of the Poisson equation, Eq. (1), one obtains

$$-\varepsilon\partial_t\nabla^2\phi = e(\partial_t n^+ - \partial_t n^-) = -e(\nabla\cdot\mathbf{j}^+ - \nabla\cdot\mathbf{j}^-), \tag{20}$$

where in the last equation, the conservation of ion densities, Eq. (3), has been used. Through integration over space (assuming a one-dimensional geometry), and using the definition of the electric field, $\mathbf{E} = -\nabla\phi$, it follows that [48,49]

$$\mathbf{I} = \varepsilon\partial_t\mathbf{E} + e\mathbf{J}, \tag{21}$$

where the constant in of integration, $\mathbf{I}$, is the total electric current density. The first term on the R.H.S in Eq. (21) is the displacement current. The second term, $\mathbf{J} = \mathbf{j}^+ - \mathbf{j}^- = 2\mathbf{j}_\rho$, is the particle current density. The displacement current was absent in the previous section because we assumed a

stationary state, but for the time-dependent case it is crucial to obtain the response to an externally applied AC electric potential. We note that by virtue of the Poisson equation, Eq. (1), the total current density is divergence-free, $\nabla \cdot \mathbf{I} = 0$, at all times. Further note that the experimentally measurable quantity is given by the total electric current. For this reason, it is the relevant quantity to calculate the impedance as shown below.

3.2. Equations for Time-periodic Perturbations of an Equilibrium Base State

Let us assume an established equilibrium solution $c_0^+(z)$, $c_0^-(z)$ and $\phi_0(z)$ for the electrolyte in the absence of the AC field, which could be caused by an additional DC field or a Nernst potential. For convenience we consider here the *charge* densities $c^\pm$. Note that $c^\pm = en^\pm$ and $\kappa^2 = 2ec_0/(\varepsilon k_B T)$. The equations for the electrostatic problem, see Eqs. (1) and (3) above, read

$$\varepsilon \partial_z^2 \phi = c^- - c^+, \tag{22}$$

$$\partial_t c^\pm = -\partial_z j^\pm, \tag{23}$$

$$j^\pm = -D^\pm \left(\partial_z c^\pm \mp c^\pm \frac{e}{k_B T} \partial_z \phi \right). \tag{24}$$

Linearization around the base state like

$$c^+ = c_0^+ + \eta C^+, \quad c^- = c_0^- + \eta C^-, \quad \phi = \phi_0 + \eta \Phi,$$

where η is a small book-keeping parameter, leads at order $\mathcal{O}(\eta^0)$ to

$$c_0^\pm = c_0 e^{\pm \frac{e\phi_0(z)}{k_B T}}, \quad \text{with } \phi_0 \text{ solution of } \varepsilon \partial_z^2 \phi_0 = c_0 \left(e^{\phi_0} - e^{-\phi_0} \right).$$

This restates that the equilibrium solution has to fulfill the classical PB equation. At order $\mathcal{O}(\eta^1)$ in the perturbations, we get

$$\varepsilon \partial_z^2 \Phi = C^- - C^+, \tag{25}$$

$$\partial_t C^\pm = D^\pm \partial_z \left(\partial_z C^\pm \mp c_0^\pm \frac{e}{k_B T} \partial_z \Phi \mp C^\pm \frac{e}{k_B T} \partial_z \phi_0 \right). \tag{26}$$

As already discussed in the general case above, taking the time derivative of Eq. (25), insertion of the linearized PNP equations, Eq. (26), and integration in z yields

$$\varepsilon\partial_z\partial_t\Phi - D^-\left(\partial_z C^- - c_0^-\frac{e}{k_B T}\partial_z\Phi - C^-\frac{e}{k_B T}\partial_z\phi_0\right) + D^+\left(\partial_z C^+ + c_0^+\frac{e}{k_B T}\partial_z\Phi + C^+\frac{e}{k_B T}\partial_z\phi_0\right) = I(t).$$

The integration constant $I(t)$ is the total electric current density. As we are interested in the response to an AC external voltage, $V(t) = V_0 e^{i\omega t}$, introducing $I(t) = I_0 e^{i\omega t}$ and $\Phi \propto e^{i\omega t}$, we arrive at

$$\left(i\omega\varepsilon + \frac{e}{k_B T}\left(D^+ c_0^+ + D^- c_0^-\right)\right)\partial_z\Phi + D^+\partial_z C^+ - D^-\partial_z C^- + \left(D^+ C^+ + D^- C^-\right)\frac{e}{k_B T}\partial_z\phi_0 = I_0. \tag{27}$$

The first term on the L.H.S is the displacement current. The remaining terms are currents due to concentration gradients and a current induced by the equilibrium potential at the membrane. All these contributions taken together yield the total current I_0 in response to the external AC field.

We are left with the problem to solve Eqs. (26) and (27) with the external voltage entering via the BC, just like in Section 2.

3.3. Impedance for an Ideally Blocking Non-conductive Membrane

The equations derived in the last section are general as they describe the first order perturbation in an electrolyte induced by an AC voltage externally imposed at some boundaries. Let us now apply them to the planar membrane geometry as sketched in Fig. 1. The membrane is assumed to be flat and located at $z = 0$. The AC voltage will be externally applied at the electrodes at $z = \pm L/2$. For simplicity, we assume that there is no additional DC electric field or Nernst potential, that is, that the equilibrium solution is given by the homogeneous solution $\phi_0 = 0$, $c_0^+ = c_0$.

First we will treat the simplest case of an ideally blocking, non-conductive membrane, $j^{\pm}(0) = 0$. We also assume equal diffusion coefficients for the positive and negative ions, $D^+ = D^- = D$. Then the above Eqs. (26) and (27) for the perturbations reduce to

$$i\omega C^{\pm} = D\partial_z\left(\partial_z C^{\pm} \mp c_0\frac{e}{k_B T}\partial_z\Phi\right), \tag{28}$$

$$\left(\mathrm{i}\omega\varepsilon + 2Dc_0\frac{e}{k_B\mathrm{T}}\right)\partial_z\Phi + D(\partial_z C^+ - \partial_z C^-) = I_0. \tag{29}$$

Due to the symmetry of our system, one has

$$\Phi(z,t) = -\Phi(-z,t), \quad \rho(z,t) = -\rho(-z,t), \quad c(z,t) = c(-z,t). \tag{30}$$

Hence it is enough to solve the problem in $z \in [-L/2,0]$. The BCs in the chosen geometry read

$$C^+(-L/2) = 0, \tag{31}$$

$$C^-(-L/2) = 0, \tag{32}$$

$$\Phi(-L/2) = -V_0/2, \tag{33}$$

$$\partial_z C^+(0) + c_0\frac{e}{k_\mathrm{B}\mathrm{T}}\partial_z\Phi(0) = 0 = j^+(0)/D, \tag{34}$$

$$\partial_z C^-(0) - c_0\frac{e}{k_\mathrm{B}\mathrm{T}}\partial_z\Phi(0) = 0 = j^-(0)/D, \tag{35}$$

$$\lambda_m\partial_z\Phi(0) = \Phi(0^+) - \Phi(0^-). \tag{36}$$

Equations (31)–(33) fix the densities and the potential at the electrodes, as has already been discussed in Section 2.1. The next two Eqs. (34) and (35) state that the membrane is non-conductive for both ion types. Finally the last equation, Eq. (36), is again the Robin-type BC describing the capacitive behavior of the membrane with the effective length scale $\lambda_m = (\varepsilon/\varepsilon_m)d$. We will use the first five BCs to fix the five integration constants of Eqs. (28) and (29). Then imposing the last condition will yield the current–voltage relation and finally the impedance.

Extracting an equation for $C_\mathrm{s} = C^+ + C^-$ by adding the two cases $\pm$ in Eq. (28) yields $\mathrm{i}\omega C_\mathrm{s} = D\partial_z^2 C_\mathrm{s}$. From the BCs $\partial_z C_\mathrm{s}(0) = 0 = \mathrm{C_s}(-1/2)$ it follows $C_\mathrm{s}(\mathrm{z}) = 0$, that is, the total density of particles (positively and negatively charged) remains homogeneous. Introducing $\rho = C^+ - C^-$ and subtracting Eq. (28) yields

$$\mathrm{i}\omega\rho = D\partial_z^2\rho + D\varepsilon\kappa^2\partial_z^2\Phi, \tag{37}$$

$$\left(\mathrm{i}\omega\varepsilon + D\varepsilon\kappa^2\right)\partial_z\Phi + D\partial_z\rho = I_0, \tag{38}$$

where we have used $c_0 e/k_\mathrm{B}T = \varepsilon\kappa^2/2$. Eq. (38) can be integrated, yielding

$$\Phi(z) = c_1 + \frac{I_0 z - D\rho(z)}{D\varepsilon\kappa^2 + \mathrm{i}\omega\varepsilon}.$$

The BCs $\rho(-L/2) = 0$, $\Phi(-L/2) = -V_0/2$ fix the constant of integration to

$$c_1 = -\frac{V_0}{2} + \frac{I_0 L/2}{D\varepsilon\kappa^2 + \mathrm{i}\omega\varepsilon}.$$

Insertion of the obtained potential into Eq. (37) for ρ yields

$$\frac{D\kappa^2 + \mathrm{i}\omega}{D}\rho = \partial_z^2 \rho. \tag{39}$$

Using again the obtained potential transforms the BC $\partial_z\rho(0) + \varepsilon\kappa^2\,\partial_z\Phi(0) = 0$ into the simpler form $\partial_z\rho(0) = \mathrm{i}(I_0\kappa^2/\omega)$. Together with $\rho(-L/2) = 0$, the solution of Eq. (39) can be given as

$$\rho(z) = \mathrm{i}\frac{I_0\kappa^2}{\beta\omega\cosh(\beta L/2)}\sinh[\beta(z + L/2)] \tag{40}$$

with the (complex) inverse length scale

$$\beta = \sqrt{\kappa^2 + \mathrm{i}\omega/D}. \tag{41}$$

The remaining BC, Eq. (36), is a jump condition at the membrane. What we have calculated above are the solutions $\Phi^{<0}$, $\rho^{<0}$ on $z \in [-L/2, 0]$. Using the symmetry of our problem, Eq. (30), one directly obtains $\Phi^{>0}$, $\rho^{>0}$ on $z \in [0, L/2]$. Imposing Eq. (36), $\lambda_m\partial_z\Phi(0) = \Phi^{>0}(0) - \Phi^{<0}(0)$, then yields

$$\begin{aligned}\lambda_m\frac{I_0 - D\partial_z\rho(0)}{D\varepsilon\kappa^2 + \mathrm{i}\omega\varepsilon} &= c_1^{>0} + \frac{-D\rho^{>0}(0)}{D\varepsilon\kappa^2 + \mathrm{i}\omega\varepsilon} - \left[c_1^{<0} + \frac{-D\rho^{<0}(0)}{D\varepsilon\kappa^2 + \mathrm{i}\omega\varepsilon}\right] \\ &= -2c_1^{<0} - 2\frac{-D\rho^{<0}(0)}{D\varepsilon\kappa^2 + \mathrm{i}\omega\varepsilon}.\end{aligned}$$

Solving for the external voltage V_0—note that it enters in the integration constant c_1 of the electric potential—one gets

$$V_0 = \frac{I_0 L}{D\varepsilon\kappa^2 + \mathrm{i}\omega\varepsilon} - 2\frac{D\rho(0)}{D\varepsilon\kappa^2 + \mathrm{i}\omega\varepsilon} + \lambda_m\frac{I_0 - D\partial_z\rho(0)}{D\varepsilon\kappa^2 + \mathrm{i}\omega\varepsilon}.$$

This is the current–voltage relation. The impedance is defined as $Z(\omega) = V(\omega)/AI(\omega) = V_0/(AI_0)$, with A the membrane area normal to

the z-direction. Using the expression for the density, Eq. (40), one arrives at the following expression for the impedance of a non-conductive membrane

$$Z = \frac{L/A}{D\varepsilon\kappa^2 + \mathrm{i}\omega\varepsilon} - i\frac{(L/A)(D\kappa^2/\omega)}{D\varepsilon\kappa^2 + \mathrm{i}\omega\varepsilon}\frac{\tanh[\beta(L/2)]}{\beta L/2} + \frac{(\lambda_m/A)(1 - i(D\kappa^2/\omega))}{D\varepsilon\kappa^2 + \mathrm{i}\omega\varepsilon}. \tag{42}$$

Let us discuss the obtained result. The first term is the contribution of the electrolyte. This can be seen by rewriting it as

$$Z_{\mathrm{B}} = \frac{1}{R_{\mathrm{B}}^{-1} + \mathrm{i}\omega C_{\mathrm{B}}} \tag{43}$$

and identifying the capacitance of the bulk, $C_{\mathrm{B}} = \varepsilon A/L$, which is in parallel with the resistance of the bulk $R_{\mathrm{B}} = (1/D\varepsilon\kappa^2)(L/A) = Lk_{\mathrm{B}}T/2Dc_0eA$. A similar interpretation holds for the term $(\lambda_m/A)/D\varepsilon\kappa^2\mathrm{i}\omega\varepsilon$ in Eq. (42), which can be written as

$$Z_{\mathrm{S}} = \frac{1}{R_{\mathrm{S}}^{-1} + i\omega C_{\mathrm{S}}}. \tag{44}$$

This is again a RC-circuit with the capacitance $C_{\mathrm{S}} = \varepsilon A/\lambda_m = \varepsilon_m A/d$ of the membrane and a resistance $R_{\mathrm{S}} = (1/D\varepsilon\kappa^2)(\lambda_m/A)$. It arises from the Robin-BC which involves the effective length scale λ_m defined in Eq. (8). One can thus recast Eq. (42) into the form

$$Z = Z_{\mathrm{B}} + Z_{\mathrm{S}} - \frac{\mathrm{i}}{\omega}\frac{D\kappa^2}{R_{\mathrm{B}}^{-1} + \mathrm{i}\omega C_{\mathrm{B}}}\left[\frac{\tanh[\beta(L/2)]}{\beta L/2} + \frac{\lambda_m}{L}\right]. \tag{45}$$

The last term in this equation, let us call it Z_{C}, is due to charging of the double layer and the membrane. This can be best seen in the limit $\lambda_D/L = 1/(\kappa L) \ll 1$, that is, when the Debye length is small compared to the system size. Then $\tanh[\beta(L/2)]/(\beta L/2) \simeq 2/(\kappa L)$ and in the prefactor, the resistance R_{B}^{-1} dominates over the capacitance. One gets

$$Z_{\mathrm{C}} \simeq \frac{1}{\mathrm{i}\omega C_{\mathrm{eff}}}, \tag{46}$$

with the effective capacitance $C_{\mathrm{eff}} = \varepsilon[A/(2\lambda_D + \lambda_m)]$. Note that the thickness of the corresponding planar capacitor is the sum of the two Debye layers thicknesses $(2\lambda_D)$ and the effective length λ_m describing the capacitive effects of the membrane.

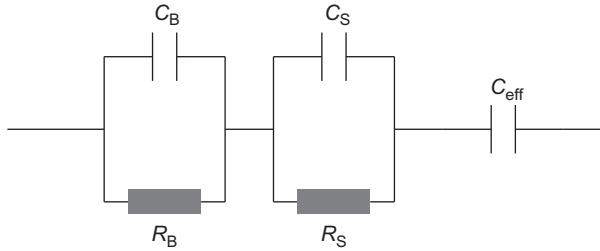

Figure 4 Effective circuit for the ideally blocking non-conductive membrane, Eq. (47): Two RC-circuits, one for the bulk and one for the membrane are in series with the effective charging capacitance of the membrane.

As shown in Fig. 4, for the blocking non-conductive membrane one effectively has an association in series of the RC-circuit of the bulk, the RC-circuit of the membrane and the effective capacitance of the charging membrane

$$Z = Z_B + Z_S + Z_C = \frac{1}{R_B^{-1} + i\omega C_B} + \frac{1}{R_S^{-1} + i\omega C_S} + \frac{1}{i\omega C_{eff}}, \qquad (47)$$

as long as $\lambda_D/L \ll 1$ holds. As $\lambda_m \simeq 200$ nm, the impedance contribution Z_S is usually small compared to the bulk resistance and can be neglected for $L \gg \lambda_m$. However, the contribution described by λ_m to the charging impedance Z_C can be of similar order as the one from the Debye layers and might even dominate the charging.

The best way to visually present the impedance is by a so-called Nyquist plot [44]. There one traces the negative imaginary part, $-\mathrm{Im}[Z(\omega)]$, of the impedance as a function of its real part, $\mathrm{Re}[Z(\omega)]$, for varying frequency ω. Nyquist plots for the full impedance, Eq. (45), and for the limit $\lambda_D/L \ll 1$, Eq. (47), are shown in Fig. 5. Panel (A) shows the case of a macroscopic system size, $L = 1$ mm. One clearly notices the RC-semi-circle terminating for high frequencies at the origin. For the given parameters one enters this semi-circle at $\omega \simeq 50$ Hz; the maximum is achieved for $\omega_{RC} = D\kappa^2 = 1$ kHz. The low frequency branch is dominated by the membrane charging capacitively at $R \simeq R_B + R_S$, thus for low frequencies one has a divergence like $(i\omega C_{eff})^{-1}$. As $\lambda_D/L \simeq 10^{-3}$, the effective circuit and the full calculation agree well.

Figure 5B shows the case of a microscopic system size, $L = 10$ μm. Here the bulk RC-signal is much less pronounced and charging dominates entirely. The full calculation (solid curve) yields a lower resistance for the charging process at low frequencies than the effective circuit obtained by the small-Debye layer approximation (dashed curve).

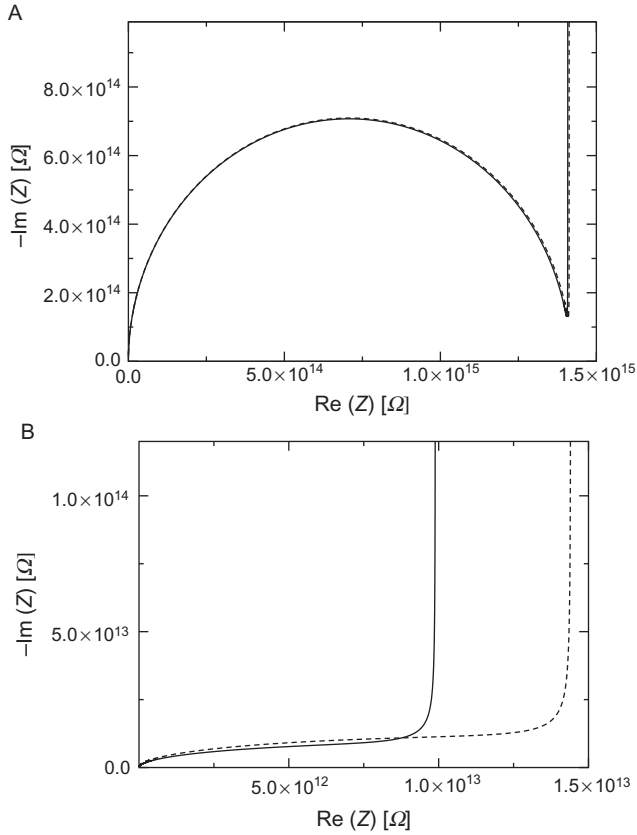

Figure 5 (A) Shows a Nyquist plot for a macroscopic system size, $L = 1$ mm. At low frequency the behavior is governed by the charging of the membrane. The semi-circle is governed by the bulk-RC-circuit. As $\lambda_D/L \simeq 10^{-3}$, the effective circuit and the full calculation agree well. (B) shows a Nyquist plot for a microscopic system, $L = 10$ μm. As L decreases, the bulk becomes less important and the RC-semi-circle less pronounced. The full calculation (solid curve) yields a lower resistance for the charging process at low frequencies than the effective circuit (dashed curve). Parameters as in Fig. 2 except for $\kappa = 10^{-6}$ m^{-1} (pure water); membrane area $A = 1$ μm^2.

3.4. Non-conductive Membrane: Effect of Unequal Diffusion Coefficients

In this section we investigate the effect of differing diffusion coefficients for the two ion species, $D^+ \neq D^-$, on the impedance of a blocking non-conductive membrane. Except for this assumption, the calculation is analogous to the one of the previous section. Equations (26) and (27) for the perturbations now read

$$\mathrm{i}\omega C^{\pm} = D^{\pm}\partial_z\left(\partial_z C^{\pm} \mp \frac{\varepsilon\kappa^2}{2}\partial_z\Phi\right), \tag{48}$$

$$\left(\mathrm{i}\omega\varepsilon + (D^{+}+D^{-})\frac{\varepsilon\kappa^2}{2}\right)\partial_z\Phi + D^{+}\partial_z C^{+} - D^{-}\partial_z C^{-} = I_0. \tag{49}$$

The BCs are still given by Eqs. (31)–(36). Since the equations for the charge densities do not decouple as before, it is useful to introduce $C = C^{+} + C^{-}$ and $\rho = C^{+} - C^{-}$ again, yielding

$$\begin{aligned}
&\mathrm{i}\omega C = \partial_z^2[\bar{D}C + \delta\rho + 2\delta\bar{c}\Phi],\\
&\mathrm{i}\omega\rho = \partial_z^2[\delta C + \bar{D}\rho + 2\bar{D}\bar{c}\Phi],\\
&(\mathrm{i}\omega\varepsilon + 2\bar{D}\bar{c})\partial_z\Phi + \delta\partial_z C + \bar{D}\partial_z\rho = I_0.
\end{aligned}$$

Here we introduced the abbreviation $\bar{c} = c_0\, e/k_B T$ as well as the average and the difference of the two diffusion coefficients

$$\bar{D} = (D^{+}+D^{-})/2, \quad \delta = (D^{+}-D^{-})/2. \tag{50}$$

Integration of the equation for the potential Φ yields

$$\Phi(z) = c_1 + \frac{I_0 z - (\delta C(z) + \bar{D}\rho(z))}{\bar{D}\varepsilon\kappa^2 + \mathrm{i}\omega\varepsilon} \quad \text{with } c_1 = -\frac{V_0}{2} + \frac{I_0 L/2}{\bar{D}\varepsilon\kappa^2 + \mathrm{i}\omega\varepsilon}.$$

Insertion into the equations for C and ρ yields a matrix equation

$$\begin{pmatrix} \mathrm{i}\omega - \left[\bar{D} - \delta^2\varepsilon\kappa^2/N\right]\partial_z^2 & -[\delta\mathrm{i}\omega\varepsilon/N]\partial_z^2 \\ -[\delta\mathrm{i}\omega\varepsilon/N]\partial_z^2\mathrm{i}\omega & -[\bar{D}\mathrm{i}\omega\varepsilon/N]\partial_z^2 \end{pmatrix}\cdot\begin{pmatrix} C \\ \rho \end{pmatrix} = 0, \tag{51}$$

where we have introduced $N = \bar{D}\varepsilon\kappa^2 + \mathrm{i}\omega\varepsilon$. Assuming solutions of the form $C, \rho \propto \mathrm{e}^{\beta z}$, Eq. (51) yields four solutions for the decay length β. In the case of equal diffusion coefficients studied previously, $\delta = 0$ and the equations are decoupled. In that case $\bar{D} = D$ and one simply gets $\beta_1^2 = \mathrm{i}\omega/D$ associated to the relaxation of the total particle density C and $\beta_2^2 = N/D\varepsilon = (D\kappa^2 + \mathrm{i}\omega)/D$ associated to the relaxation of ρ, see Eq. (39). In the case of unequal diffusion coefficients, the equations are coupled and the general solutions are

$$\beta_{1,2}^2 = \frac{\mathrm{i}\omega\bar{D} + \left(\bar{D}^2 - \delta^2\right)\kappa^2/2 \mp \sqrt{(\kappa^2/2)^2\left(\bar{D}^2 - \delta^2\right)^2 - \delta^2\omega^2}}{\left(\bar{D}^2 - \delta^2\right)}. \tag{52}$$

Here the minus sign applies to β_1 and the plus sign to β_2. Consequently, Eq. (51) is solved by the ansatz

$$\begin{pmatrix} C \\ \rho \end{pmatrix} = \sum_{i=1,2} \left[A_i \begin{pmatrix} E_i \\ 1 \end{pmatrix} \sinh[\beta_i(z+L/2)] + B_i \begin{pmatrix} E_i \\ 1 \end{pmatrix} \cosh[\beta_i(z+L/2)] \right]$$

with the eigenvectors given by

$$E_i = \frac{[\delta \mathrm{i}\omega\varepsilon/N]\beta_i^2}{\mathrm{i}\omega - \left[\bar{D} - \delta^2\varepsilon\kappa^2/N\right]\beta_i^2}.$$

The effective BCs read: $\partial_z C(0) = 0$ and $\partial_z \rho(0) = \mathrm{i}(2\bar{c}I_0/\omega\varepsilon)$ at $z = 0$; $C(-L/2) = 0$ and $\rho(-L/2)$ at $z = -L/2$. The last two BCs yield $E_1B_1 + E_2B_2 = 0$ and $B_1 + B_2 = 0$. As $E_1 \neq E_2$ this implies $B_1 = 0 = B_2$, that is, the cosh-contributions in the solution vanish. After some algebra one obtains

$$\rho = \mathrm{i}\frac{I_0\kappa^2}{\omega}\frac{E_1E_2}{E_2 - E_1}\left[\frac{\sinh[\beta_1(z+L/2)]}{E_1\beta_1\cosh(\beta_1 L/2)} - \frac{\sinh[\beta_2(z+L/2)]}{E_2\beta_2\cosh(\beta_2 L/2)}\right],$$
$$C = \mathrm{i}\frac{I_0\kappa^2}{\omega}\frac{E_1E_2}{E_2 - E_1}\left[\frac{\sinh[\beta_1(z+L/2)]}{\beta_1\cosh(\beta_1 L/2)} - \frac{\sinh[\beta_2(z+L/2)]}{\beta_2\cosh(\beta_2 L/2)}\right].$$

Using the Robin-type BC, Eq. (36), and once again the symmetry of the problem one gets

$$\lambda_m \frac{I_0 - (\delta\partial_z C(0) + \bar{D}\partial_z\rho(0))}{2\bar{D}\bar{c} + \mathrm{i}\omega\varepsilon} = -2c_1^{<0} - 2\frac{-(\delta C^{<0}(0) + \bar{D}\rho^{<0}(0))}{2\bar{D}\bar{c} + \mathrm{i}\omega\varepsilon}.$$

Solving for V_0, insertion of the obtained solutions for C and ρ and applying $Z = V_0/(I_0A)$ one obtains the impedance

$$\begin{aligned} Z = {} & \frac{L/A}{\bar{D}\varepsilon\kappa^2 + \mathrm{i}\omega\varepsilon} + \frac{(\lambda_m/A)(1 - \bar{D}\mathrm{i}(\kappa^2/\omega))}{\bar{D}\varepsilon\kappa^2 + \mathrm{i}\omega\varepsilon} \\ & - \mathrm{i}\frac{2\kappa^2/A}{(\bar{D}\kappa^2 + \mathrm{i}\omega)\omega\varepsilon}\frac{E_1E_2}{E_2 - E_1}\left(\delta + \frac{\bar{D}}{E_1}\right)\frac{\tanh[\beta_1 L/2]}{\beta_1} \\ & + \mathrm{i}\frac{2\kappa^2/A}{(\bar{D}\kappa^2 + \mathrm{i}\omega)\omega\varepsilon}\frac{E_1E_2}{E_2 - E_1}\left(\delta + \frac{\bar{D}}{E_2}\right)\frac{\tanh[\beta_2 L/2]}{\beta_2}. \end{aligned} \tag{53}$$

The first two contributions are already familiar to us, they stem from the bulk and the Stern-like description of the membrane. Note that $\bar{D}$ enters instead of D.Let us discuss the newly arising terms. As an expansion in $\lambda_D/L \ll 1$ is a bit tedious, let us consider only the simpler limit $\kappa \to \infty$. Equation (52) for β_1^2 has a minus sign in front of the square root, the two κ-terms cancel and

$$\beta_1^2 = \frac{\mathrm{i}\omega\bar{D}}{\left(\bar{D}^2 - \delta^2\right)} \to \beta_1 = \pm\sqrt{\mathrm{i}\omega/D_{\mathrm{eff}}} \tag{54}$$

with $D_{\mathrm{eff}} = (\bar{D}^2 - \delta^2)/\bar{D}$. For β_2^2 one has the plus sign in front of the square root, the terms in κ^2 dominate and one simply gets $\beta_2 = \pm\kappa$. For the eigenvectors to leading order one has $E_1 = (\bar{D}^2 - \delta^2)\kappa^2/\delta\mathrm{i}\omega$, $E_2 = -(1/E_1)$ and $(E_1E_2/E_2 - E_1)(\delta + (\bar{D}/E_1)) = \mathrm{i}\omega\delta^2/\kappa^2(\bar{D}^2 - \delta^2)$, $(E_1E_2/E_2 - E_1)(\delta + (\bar{D}/E_2)) = -\bar{D}$.

Consequently, the last term in Eq. (53) exactly reduces to the Debye-layer part of the charging contribution. Finally one obtains at leading order in λ_D

$$Z = \bar{Z}_{\mathrm{B}} + \bar{Z}_{\mathrm{S}} + Z_{\mathrm{C}} + Z_{\mathrm{W}} \tag{55}$$

with

$$Z_{\mathrm{W}} = \frac{2\lambda_D^2}{\bar{D}\varepsilon A/L}\frac{\delta^2}{\left(\bar{D}^2 - \delta^2\right)}\frac{\tanh[\beta_1 L/2]}{\beta_1 L}. \tag{56}$$

The first two terms are the RC-contributions of the bulk and the membrane (note that $\bar{D} = (D^+ + D^-)/2$ enters instead of D). The charging capacitance Z_{C} of the membrane is unchanged. The last term is the so-called Warburg impedance, with $\beta_1 = \sqrt{\mathrm{i}\omega/D_{\mathrm{eff}}}$ and $D_{\mathrm{eff}} = (\bar{D}^2 - \delta^2)/\bar{D}$. Note that this contribution is only present for unequal diffusion coefficients $\delta = (D^+ - D^-)/2 \neq 0$. It is proportional to λ_D^2 at leading order.[1]

The effective circuit corresponding to the obtained impedance is shown in Fig. 6. The contribution Z_{W} has been first described by Warburg [50,51] for electrochemical systems; in a nutshell, it arises from damped concentration oscillations close to an interface, here the membrane. We note however, that with typical differences in diffusion coefficients $D^+/D^- = 0.1$–10, a Nyquist

[1] For simplicity, we used the limit $\kappa \to \infty$ to derive this term. Taking this limit strictly, the contribution would vanish—as then both charge types diffuse infinitely rapidly across the zero-thickness Debye-layer. In real systems, however, κ remains always finite and thus one should include the leading order contribution, Z_W, in the impedance.

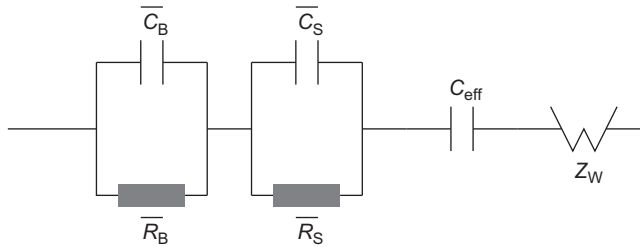

Figure 6 Effective circuit for the ideally blocking non-conductive membrane with differing diffusion coefficients, Eq. (55): Two RC-circuits, one for the bulk and one for the membrane are in series with the effective charging capacitance and a Warburg resistance.

plot of Eq. (55) is indistinguishable from Fig. 5 obtained for equal diffusion coefficients. This is due to the fact that in the geometry under investigation, the charging of the membrane is highly dominating the low-frequency behavior as it is proportional to ω^{-1}. Nevertheless, experiments often display a Warburg-like impedance at low frequencies, see, for example, Ref. [46]. In the next section we will investigate the case of a slightly conductive ion-selective membrane and will find that in this case one indeed obtains a Warburg impedance. We thus postpone a discussion of Z_W to the next section.

3.5. Impedance for an Ideally Non-blocking Conductive Membrane

For many applications it is interesting to account for a small but nonzero membrane conductivity. This is important for instance in the context of the characterization of ion channel proteins or pumps embedded in a lipid membrane using impedance spectroscopy. In contrast to Section 2.1, where we discussed the effects of a DC voltage on a conductive membrane that lets pass both types of charged ions ($G^+ = G^- = G$), here we will treat the case of a *selective membrane*, which lets pass only the positive ions. Thus, we assume a linearized relation $j^+ = G^+ \Delta\mu^+$ where G^+ is the effective conductance per unit area. The negative ions are not allowed to pass the membrane, hence $j^- = 0$ or effectively $G^- = 0$. This situation is relevant for biomembranes, where ion channels allow the passage of positively charged ions like Na^+ or K^+, but not of negatively charged ions like Cl^- which are typically larger.

To simplify the analysis, we will not describe the structure of the Debye layers as explicitly as in the previous sections. Instead we rely on two known approximations used in the study of electrochemical systems:

(i) the bulk is to a good approximation *locally* electroneutral. More precisely, deviations from electroneutrality occur only in the third order in an expansion of λ_D/L, which is very small for usual system sizes. This result can be obtained using a matched asymptotic expansion [33]. Consequently, we will assume for all z, $\rho(z) = 0$, or $C(z) = C^+(z) = C^-(z)$ for the perturbation of the charge densities.

(ii) Although we do not treat the Debye layers explicitly, we still impose effective BC for the electrochemical potential at the membrane. Thus, we implicitly assume that the electrochemical potential is continuous across the Debye layers.

We keep the geometry as before, that is, a flat membrane located at $z = 0$ with given AC voltage V_0 at the electrodes located at $z = \pm L/2$. We again assume that there is no additional DC field or Nernst potential, and equal diffusion coefficients[2] for positive and negative ions. Using the above-discussed approximations, we obtain

$$\mathrm{i}\omega C = D\partial_z^2 C, \tag{57}$$

$$\left(\mathrm{i}\omega\varepsilon + D\varepsilon\kappa^2\right)\partial_z\Phi = I_0. \tag{58}$$

Equation (58) is again easily integrated for $z \in [-L/2, 0]$ and together with the BC $\Phi(-L/2) = -V_0/2$ one gets

$$\Phi(z) = \frac{I_0(z + L/2)}{\mathrm{i}\omega\varepsilon + D\varepsilon\kappa^2} - V_0/2.$$

In addition we need three more BCs, namely

$$C(-L/2) = 0, \tag{59}$$

$$D(\partial_z C(0) - \bar{c}\partial_z\Phi(0)) = j^- = 0, \tag{60}$$

$$D(\partial_z C(0) + \bar{c}\partial_z\Phi(0)) = j^+ = \frac{G^+}{e}\left(\frac{\kappa_B T}{c_0}[C]_0 + e[\Phi]_0\right), \tag{61}$$

where $[C]_0 = C(0^+) - C(0^-)$ and analogously for $[\Phi]_0$. The second condition is the no-flux condition for the anions. The third condition states that the bulk current of cations equals the current through the membrane, and is assumed to follow Ohm's law. From Eqs. (57), (59), and (60), we obtain the following frequency dependent ion density distribution

[2] Note that in case of unequal diffusion coefficients, one gets a contribution like $\partial_z C$ in Eq. (58). The subsequent calculations can still be performed in a completely analogous way.

$$C(z) = \frac{\varepsilon\kappa^2 I_0}{2\alpha(\mathrm{i}\omega\varepsilon + D\varepsilon\kappa^2)\cosh(\alpha L/2)} \sinh(\alpha(z + L/2)),$$

where $\alpha = \sqrt{\mathrm{i}\omega/D}$ is of Warburg-type, cf. Eq. (54). Note that here the Warburg impedance arises from breaking the cation/anion symmetry, due to differences in membrane conductivities rather than due to differences in their diffusion coefficients as in the previous section. Also note that although the membrane is non-conductive for the anions, this is a collective effect in which both types of moving charges participate.

Finally, we use the BC for the cationic current, Eq. (61), to solve for the voltage V_0 and obtain the impedance via $Z = V_0/(I_0 A)$ as before

$$Z = Z_{\mathrm{B}} + \frac{D\kappa^2/(G^+ A)}{D\kappa^2 + \mathrm{i}\omega} + \frac{k_{\mathrm{B}}\mathrm{T}\kappa^2/(ec_0 A)}{\mathrm{i}\omega + D\kappa^2} \frac{\tanh(\alpha L/2)}{\alpha}. \tag{62}$$

Here we already have identified the bulk circuit, it is present as in the previous cases. The second term is the membrane contribution. It can be written as

$$Z_{\mathrm{M}} = \frac{1}{R_{\mathrm{M}}^{-1} + \mathrm{i}\omega C_{\mathrm{M}}}, \tag{63}$$

with the membrane's resistance, $R_{\mathrm{M}} = 1/(G^+ A)$, and capacitance, $C_{\mathrm{M}} = G^+ A/D\kappa^2$. The third term is the Warburg impedance, reading

$$Z_{\mathrm{W}} \simeq \frac{2\lambda_D^2}{D\varepsilon A/L} \frac{\tanh(\sqrt{\mathrm{i}\omega/D}L/2)}{\sqrt{\mathrm{i}\omega/D}L} \tag{64}$$

for small ω. Note that it is of the same form as Eq. (56) obtained for unequal diffusion coefficients, except for that in the latter appears an additional factor containing the diffusion coefficients.

We can conclude that as a result of the ionic membrane selectivity, a Warburg impedance arises. Figure 7 shows the effective circuit. A Nyquist plot is given in Fig. 8. One can identify the typical shape of a Warburg impedance for low frequencies: namely, for decreasing frequencies, on leaving the RC-signal of the bulk $-\mathrm{Im}[Z(\omega)]/\mathrm{Re}[Z(\omega)]$ acquires a slope of 45°. Finally, due to the finite system size $\mathrm{Im}[Z(\omega)]$ vanishes for $\omega \to 0$.

As already stated above, the calculation in this Section 3.5 is over-simplified. By assuming that the electrochemical potential is continuous across the Debye layers, there is no explicit contribution from the charging of the Debye layers to the impedance. Hence λ_m, which is important for the charging, does not enter—indeed we did not even use the Robin-type condition. As the membrane is conductive, at least for the cations, charging

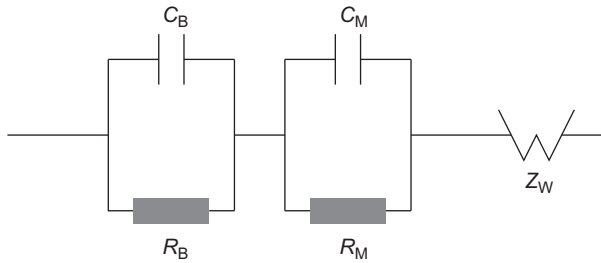

Figure 7 Effective circuit for the ideally blocking and selectively conductive membrane, Eq. (62): Two RC-circuits, one for the bulk and one for the membrane are in series with a Warburg resistance, caused by the ion selectivity of the membrane.

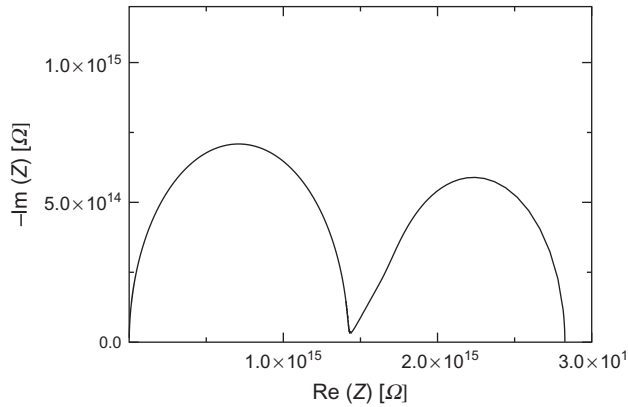

Figure 8 Nyquist plot for a selectively conducting membrane. At high frequencies one has an RC-semi-circle, which is either dominated by the bulk or by the membrane, depending on the membrane conductance and the dimensions of the system. The low-frequency behavior is governed by the Warburg impedance. Parameters as for Fig. 2 except for: $L = 1$ mm; $\kappa = 10^{-6}$ m^{-1} (pure water); $A = 1$ μm^2.

of the Debye layers is of minor importance for the overall impedance. With a proper treatment of the charging of the Debye layers, using a matched asymptotic calculation, the Robin-type condition will reoccur to match the two solutions and will reintroduce the length scale λ_m into the problem.

4. Conclusion

The study and theoretical description of the effects induced by electric fields on lipid membranes in an electrolyte is a vast, challenging, and far from fully explored problem, which is of relevance for many applications in biotechnology.

In this review, we have presented a theoretical framework to understand some of these effects in the simple case of a planar geometry. We have seen the importance of capacitive effects, occurring as a result of charge accumulation in the vicinity of the membrane, leading to renormalized elastic moduli and to membrane instabilities. We also have analyzed the flow fields which can be induced by currents due to small membrane conductivities. We discussed these effects only for time-independent (DC) electric fields, that is, in the steady-state regime.

Clearly, time-dependent electric fields lead to capacitive charging of the membrane and to time-dependent membrane dynamics. The capacitive charging can be described in two ways: the first approach is based on the leaky dielectric model developed by Taylor [52]. This approach is explained and illustrated in the contribution of P. Vlahovska [53]. One advantage of such an approach is that it captures the main physical effects associated with capacitive charging without the complexity of models which deal explicitly with the ion concentration fields. For this reason, it is useful to describe for instance the complex shape changes occurring in closed lipid vesicles [8].

The second approach, which we used in this work, is based on the electrokinetic PNP equations. This more refined level of description includes ion concentration fields, and therefore it is useful to describe specific effects associated for instance with the ion transport in ion channels or for effects occurring in low salt conditions. It is also needed to describe more precisely the capacitive charging, which as we have shown here includes several contributions coming from the bulk, the membrane impedance and the Debye layers themselves. In this review, we have tried to illustrate the strength of this approach for quantifying the impedance of a membrane-electrolyte system. In particular, we have shown how effective circuits used to interpret experimental data can be directly derived by this method. The membrane selectivity with respect to ion species is crucial to understand the conduction properties of membranes with embedded ion channels. We hope that our work will motivate further experimental and theoretical investigations in this field.

ACKNOWLEDGMENTS

We would like to thank particularly Martin Z. Bazant and Petia Vlahovska for many helpful discussions and access to unpublished work. We would also like to thank J. Prost, J. F. Joanny, P. Bassereau, L. Dinis, G. Toombes and S. Aimon for many inspiring discussions, and the ANR Artif-Neuron for funding. F. Z. thanks the DFG for partial funding via IRTG 1642 Soft Matter Science.

Appendix. Robin-type BC

In brief, this BC can be motivated for a flat membrane as follows: since the membrane is assumed to bear no fixed charges, the normal components of the electric displacement are continuous at the two interfaces between the membrane and the electrolyte,

$$\varepsilon\partial_z\phi(z=\pm d/2)=\varepsilon_m\partial_z\phi_m(z=\pm d/2), \tag{A.1}$$

where ϕ_m is the electric potential inside the membrane. Since the electric field $E_m=-\partial_z\phi_m$ is constant (to leading order) inside the membrane, the integral of the inside field can be written in the following way

$$E_m d=\int_{-d/2}^{d/2}E_m\mathrm{d}z=-[\phi_m(d/2)]-\phi_m(-d/2)]=-[\phi(d/2)-\phi(-d/2)],$$

where in the last step we used the continuity of the potential at the membrane surface. Together with Eq. (A.1) this yields

$$\lambda_m\partial_z\phi(z=\pm d/2)=\phi(d/2)-\phi(-d/2). \tag{A.2}$$

If we take the limit $d\to 0$ while keeping $\lambda_m=(\varepsilon/\varepsilon_m)d$ constant, one obtains Eq. (7) in the particular case of $h=0$ and $\mathbf{n}=\hat{z}$. The same derivation holds for the case of a slightly perturbed membrane surface $h(\mathbf{r}_\perp)$, where $\mathbf{r}_\perp$ is the in-plane vector.

REFERENCES

[1] U. Seifert, Configurations of fluid membranes and vesicles, Adv. Phys. 46 (1997) 13.
[2] D. Andelman, in: R. Lipowsky, E. Sackmann (Eds.), Handbook of Biological Physics vol. 1A, Elsevier, Amsterdam, 1995.
[3] E. Neumann, A.E. Sowers, C.A. Jordan, Electroporation and Electro-fusion in Cell Biology, Plenum Press, New York, 1989.
[4] P.T. Vernier, Y. Sun, M. Gundersen, Nanoelectropulse-driven membrane perturbation and small molecule permeabilization, BMC Cell Biol. 7 (2006) 37.
[5] H. Mekid, L.M. Mir, In vivo cell electrofusion, Biochim. Biophys. Acta Gen. Subj. 1524 (2000) 118–130.
[6] M. Staykova, R. Lipowsky, R. Dimova, Membrane flow patterns in multicomponent giant vesicles induced by alternating electric fields, Soft Matt. 4 (2008) 2168.
[7] R. Dimova, N. Bezlyepkina, M.D. Jordo, R.L. Knorr, K.A. Riske, M. Staykova, et al. Vesicles in electric fields: Some novel aspects of membrane behavior, Soft Matt. 5 (2009) 3201.

[8] P.M. Vlahovska, R.S. Graci, S. Aranda-Espinoza, R. Dimova, Electro-hydrodynamic model of vesicle deformation in alternating electric fields, Biophys. J. 96 (2009) 4789–4803.
[9] P. Peterlin, S. Svetina, B. Zeks, The prolate-to-oblate shape transition of phospholipid vesicles in response to frequency variation of an AC electric field can be explained by the dielectric anisotropy of a phospholipid bilayer, J. Phys.: Cond. Matt. 19 (2007) 136220.
[10] A. Ajdari, Pumping liquids using asymmetric electrode arrays, Phys. Rev. E 61 (2000) R45–R48.
[11] A. González, A. Ramos, N.G. Green, A. Castellanos, H. Morgan, Fluid flow induced by nonuniform AC electric fields in electrolytes on micro-electrodes. ii. a linear double-layer analysis, Phys. Rev. E 61 (2000) 4019–4028.
[12] B. Hille, Ion Channels of Excitable Membranes, Sinauer Press, Sunder-land, 2001.
[13] B. Alberts, Molecular Biology of the Cell, Garland, New York, 2002.
[14] J.B. Manneville, P. Bassereau, D. Lévy, J. Prost, Activity of transmembrane proteins induces magnification of shape fluctuations of lipid membranes, Phys. Rev. Lett. 82 (1999) 4356.
[15] J.B. Manneville, P. Bassereau, S. Ramaswamy, J. Prost, Active membrane fluctuations studied by micropipet aspiration, Phys. Rev. E 64 (2001) 021908.
[16] M.D.E.A. Faris, D. Lacoste, J. Pécréaux, J.-F. Joanny, J. Prost, P. Bassereau, Membrane tension lowering induced by protein activity, Phys. Rev. Lett. 102 (2009) 038102.
[17] D. Lacoste, M. Cosentino Lagomarsino, J.-F. Joanny, Fluctuations of a driven membrane in an electrolyte, Europhys. Lett. 77 (2007) 18006.
[18] D. Lacoste, G.I. Menon, M.Z. Bazant, J.F. Joanny, Electrostatic and electrokinetic contributions to the elastic moduli of a driven membrane, Eur. Phys. J. E 28 (2009) 243–264.
[19] F. Ziebert, M.Z. Bazant, D. Lacoste, Effective zero-thickness model for a conductive membrane driven by an electric field, Phys. Rev. E 81 (2010) 031912.
[20] F. Ziebert, D. Lacoste, A Poisson-Bolzmann approach for a lipid membrane in an electric field, New J. Phys. 12 (2010) 095002.
[21] M. Winterhalter, W. Helfrich, Effect of surface-charge on the curvature elasticity of membranes, J. Phys. Chem. 92 (1988) 6865–6867.
[22] H. Lekkerkerker, Contribution of the electric double-layer to the curvature elasticity of charged amphiphilic monolayers, Physica A 159 (1989) 319–328.
[23] M. Winterhalter, W. Helfrich, Bending elasticity of electrically charged bilayers - coupled monolayers, neutral surfaces, and balancing stresses, J. Phys. Chem. 96 (1992) 327–330.
[24] T. Chou, M. Jaric, E. Siggia, Electrostatics of lipid bilayer bending, Biophys. J. 72 (1997) 2042–2055.
[25] T. Ambjörnsson, M.A. Lomholt, P.L. Hansen, Applying a potential across a biomembrane: Electrostatic contribution to the bending rigidity and membrane instability, Phys. Rev. E 75 (2007) 051916.
[26] J. Prost, R. Bruinsma, Shape fluctuations of active membranes, Europhys. Lett. 33 (1996) 321.
[27] S. Ramaswamy, J. Toner, J. Prost, Nonequilibrium fluctuations, traveling waves, and instabilities in active membranes, Phys. Rev. Lett. 84 (2000) 3494.
[28] R.J. Hunter, Foundations of Colloid Science, Oxford University Press, Oxford, 2001.
[29] V. Kumaran, Electrohydrodynamic instability of a charged membrane, Phys. Rev. E 64 (2001) 011911.
[30] M. Leonetti, E. Dubois-Violette, F. Homblé, Pattern formation of stationary transcellular ionic currents in fucus, Proc. Natl. Acad. Sci. USA 101 (2004) 10243.

[31] E.M. Itskovich, A.A. Kornyshev, M.A. Vorotyntsev, Electric current across the metal-solid electrolyte interface. i. direct current, current-voltage characteristic, Phys. Status Solidi A 39 (1977) 229–238.
[32] K. Chu, M. Bazant, Electrochemical thin films at and above the classical limiting current, SIAM J. Appl. Math. 65 (2005) 1485–1505.
[33] M.Z. Bazant, K. Thornton, A. Ajdari, Diffuse charge dynamics in electrochemical systems, Phys. Rev. E 70 (2004) 021506.
[34] P. Sens, H. Isambert, Undulation instability of lipid membranes under an electric field, Phys. Rev. Lett. 88 (2002) 128102.
[35] F. Brochard, J.F. Lennon, Frequency spectrum of the flicker phenomenon in erythrocytes, J. Phys. (Paris) 36 (1975) 1035.
[36] M.Z. Bazant, T.M. Squires, Induced-charge electrokinetic phenomena: Theory and microfluidic applications, Phys. Rev. Lett. 92 (2004) 066101.
[37] S. Lecuyer, G. Fragneto, T. Charitat, Effect of an electric field on a floating lipid bilayer: A neutron reflectivity study, Eur. Phys. J. E 21 (2006) 153–159.
[38] J. Daillant, E. Bellet-Amalric, A. Braslau, T. Charitat, G. Fragneto, F. Graner, et al. Structure and fluctuations of a single floating lipid bilayer, Proc. Natl. Acad. Sci. USA 102 (2005) 11639–11644.
[39] N. Gov, Membrane undulations driven by force fluctuations of active proteins, Phys. Rev. Lett. 93 (2004) 268104.
[40] S. Sankararaman, G.I. Menon, P.B. Sunil Kumar, Electrostatic and electrokinetic contributions to the elastic moduli of a driven membrane, Phys. Rev. E 66 (2002) 031914.
[41] D. Lacoste, A. Lau, Dynamics of active membranes with internal noise, Europhys. Lett. 70 (2005) 418.
[42] H.-Y. Chen, Internal states of active inclusions and the dynamics of an active membrane, Phys. Rev. Lett. 92 (2004) 168101.
[43] M.A. Lomholt, Mechanics of nonplanar membranes with force-dipole activity, Phys. Rev. E 73 (2006) 061913.
[44] J.O.M. Bockris, A.K.H. Reddy, Modern Electrochemistry, Kluwer Academic/Plenum Press, New York, 2000.
[45] G. Wiegand, N. Arribas-Layton, H. Hillebrandt, E. Sackmann, P. Wagner, Electrical properties of supported lipid bilayer membranes, J. Phys. Chem. B 106 (2002) 4245–4254.
[46] E.K. Schmitt, C. Weichbrodt, C. Steinem, Impedance analysis of gramicidin d in pore-suspending membranes, Soft Matt. 5 (2009) 3347–3353.
[47] I. Rubinstein, B. Zaltzman, A. Futerman, V. Gitis, V. Nikonenko, Reexamination of electrodiffusion time scales, Phys. Rev. E 79 (2009) 021506.
[48] J.D. Jackson, Classical Electrodynamics, Wiley, New York, 1999.
[49] D. Andrieux, P. Gaspard, Stochastic approach and fluctuation theorem for ion transport, J. Stat. Mech. Theor. Exp. 2009 (2009) P02057.
[50] E. Warburg, Ueber das verhalten sogenannter unpolarisirbarer elektro-den gegen wechselstrom, Ann. Phys. (Lpz.) 67 (1899) 493(Ser. 3).
[51] E. Warburg, Polarization capacity of platinum, Ann. Phys. 6 (1901) 125.
[52] J.R. Melcher, G.I. Taylor, Electrohydrodynamics: a review of the role of interfacial shear stresses, Annu. Rev. Fluid Mech. 1 (1969) 111–146.
[53] P. Vlahovska, Adv. Planar Lipid Bilayers Liposomes 12(2010) (1969) 111–146.